OPEN ACCESS

Scholars International Journal of Chemistry and Material Sciences

Abbreviated Key Title: Sch Int J Chem Mater Sci
ISSN 2616-8669 (Print) |ISSN 2617-6556 (Online)
Scholars Middle East Publishers, Dubai, United Arab Emirates
Journal homepage: http://saudijournals.com

Original Research Article

Computational Based Study of Thiomethyl Substituents' Position on Quinoline for Inhibition of Aluminium Corrosion in Hydrochloric Acid Solution

A.M. Usman[1]*, A.A. Muhammad[2], Sulaiman Tijjani Nasiru[1], Abdulrahman Muhammad Haris[3], Muzammil Usman[4]

[1]Department of Applied Chemistry, Federal University of Technology Babura, Jigawa State, Nigeria, P.M.B 2022 Babura, Nigeria
[2]Department of Pure and Industrial Chemistry, Bayero University, P.M.B. 3011, Kano, Nigeria
[3]Prince Abdulmuhsin General hospital, Alula Madina, Saudi Arabia
[4]Department of Chemistry, Federal College of Education (Technical) Bichi, Kano, Nigeria.

DOI: https://doi.org/10.36348/sijcms.2025.v08i06.005 | **Received:** 09.08.2025 | **Accepted:** 07.10.2025 | **Published:** 26.12.2025

***Corresponding author:** A.M. Usman
Department of Applied Chemistry, Federal University of Technology Babura, Jigawa State, Nigeria, P.M.B 2022 Babura, Nigeria

Abstract

Quantum chemical study of some thiomethyl quinolines on inhibition of aluminium corrosion in hydrochloric acid and effect of thiomethyl group at 5,6 and 8 position on quinoline was investigated theoretically with the aid of material studio using density functional theory (DFT). The simulations were performed by means of the DFT electronic program DMol^3 using the Mulliken population analysis in the Material Studio. DMol^3 permits analysis of the electronic structures and energies of molecules, solids and surfaces. The analysis of the quantum chemical parameters, the adsorption parameters form the simulation of the molecules, the Mulliken and Hirshfeld values of the fukui indices for the three molecules of the 5-TMQ (5-thiomethylquinoline), 6-TMQ (6-thiomethylquinoline) and 8-TMQ (8-thiomethylquinoline) indicated that all the three molecules exhibits very high potential for inhibition of aluminium corrosion in HCl environment, with 8-TMQ being the best among all. The most popular parameters which play a prominent role are the eigen values of the highest occupied molecular orbital (HOMO) and lowest unoccupied molecular orbital (LUMO), the HOMO-LUMO gap (ΔE), chemical hardness and softness, electro-negativity and the number of electrons transferred from inhibitor molecule to the metal surface. All the molecules showed a very good corrosion inhibition tendency, however, 8-TMQ molecule gives better aluminium corrosion inhibition potential than other two molecules. The orientation of the thiomethyl substituent on the core quinoline was found to be responsible for intra-molecular hydrogen bonding which leads to weaker attraction to the aluminium surface for the 6-TMQ and 5-TMQ molecules hence lower corrosion inhibition tendency than 8-TMQ molecule despite having the same molecular mass.

Keywords: Hydroxyquinoline, Aluminium, Corrosion, Inhibition Efficiency Substituent, Position, Quantum Chemical Parameter, Influence.

1.0 INTRODUCTION

Just like iron, aluminium is globally widespread in application, and as one of the less noble non-ferrous metal it has a strong tendency to undergo all forms of corrosion in aggressive environments [1]. Despite having a protected oxides films, it do undergo passivation (gradual removal of the protective oxides). The extraction of aluminium from its ore (bauxite) is virtually energy extensive and economically expensive necessitating the needs for protection against severe corrosion attack in corrosive environment [2]. Hydrochloric acid is a common acidic medium for used by so many industries for many purposes, because it is more economical, efficient and less troublesome compared to other mineral acids. In the actual facts, Cl- from various sources including neutral salts, has the ability to cause pitting corrosion at vulnerable spots of passive film-protected non-ferrous metal [3].

Many experimental methods and modern surface characterization tools have been created to evaluate and characterize the performance of corrosion inhibitors for metals and alloys [4]. These methodologies are often expensive, time consuming and tedious. Computational methods have already proven to be very useful in determining the inhibitors molecular structure

and elucidating its electronic properties and reactivity. The aim of assessing the efficiency of a corrosion inhibitor, with the help of computational chemistry tools, is to search for compounds with desired properties, using mathematically quantified and computerized forms [5]. The development of DFT, force fields and molecular dynamic (MD) simulations, abolition, semi-empirical and Hartree-Fock model approaches provides potential solutions [5]. The pioneering work of Hohenberg and Kohn (1964) [6], and Kohn and Sham (1965) [6], has made DFT one of the more popular tools among computational chemical methods, because it focuses on the electron density P(r) as the carrier of all information in the molecular ground state, rather than on a single-electron wave function [6]. Several molecular parameters and descriptors widely used in the molecular characterization of corrosion inhibitors' effectiveness on the metal surfaces have been derived from DFT. Computational chemistry serve as a modern tool in developing novel molecules for the protection of metals and alloys that are important engineering contributors [7].

Thiomethylquinolines are nitrogenous bicyclic heterocyclic compounds with molecular formula of $C_{10}H_7NS$, as such it is expected to show a reasonable effectiveness against metallic corrosion because of its association with high electron density (10-π and 2-nonbonding electrons). Quinoline derivatives containing polar substituent such as thiomethyl group can effectively adsorb and form highly stable chelating complexes with surface metallic atoms through coordination bonding [8]. The available studies for corrosion inhibition of quinoline molecules focuses on the nature and type of functional groups (being substituted or non-substituted) attached to the molecule in use. To our knowledge, this is the first investigation for the effect of position of substituent groups in corrosion inhibition for aluminium in acidic environment by computational method. However, aside from aromaticity, functional group and the type of substituent, corrosion inhibition efficiency of heterocyclic compound can also be influence by the nature and position of substituent attached to the molecule. This study is aimed at justifying the claim, being very scanty or non from the literature. The structures of the quinolines having thiomethyl substituent at position five, six and eight respectively shown in figure 1, 2 and 3 were utilized in this research.

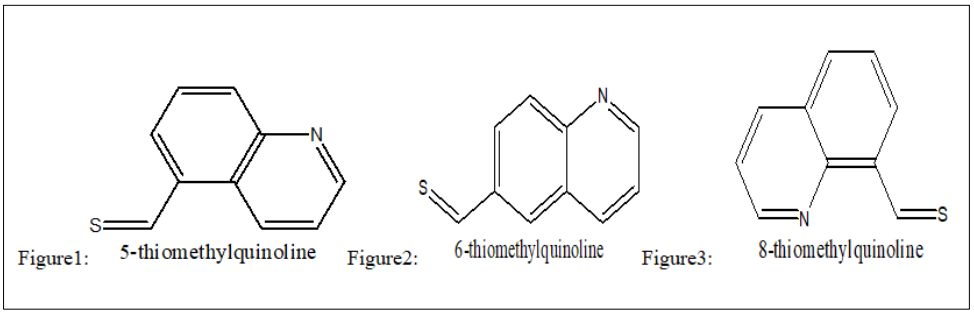

Figure1: 5-thiomethylquinoline Figure2: 6-thiomethylquinoline Figure3: 8-thiomethylquinoline

2.0 METHODOLOGY

2.1 Materials

The materials and instruments used in this research include: aluminium, Thiomethyl-quinoline derivatives and Dell Computer Core i5 16G RAM of high resolution, install with Material studio Version 2017.

2.2 Procedures

2.2.1 Sketching of Molecules

Materials Studio icon on the desktop was double-clicked to start the program. New project dialogue was opened and named according to structure of interest shown in figure 1, 2 and 3 (5-TMQ, 6-TMQ, 8-TMQ). This starts by sketching a ring, followed by the remaining parts of the molecule to produce the substituted quinoline molecule. This was achieved by choosing File, followed by New, from the menu bar to open the New Document dialogue.3D Atomistic was selected from the options and the Ok button was clicked [9]. To sketch a ring and/or cyclic compounds, four, five and six membered rings are provided as templates in Materials Studio and can be sketched easily using the Sketch Ring tool. The Sketch Ring button was clicked on the Sketch toolbar. The cursor changed to the sketching cursor, with a number 6 in the centre of a ring denoting that a six-membered ring was drawn when clicking in the new document. The next step was to place the phenyl ring in the 3D Atomistic document. By default, the Sketch Ring tool generates a ring of carbons connected by single bonds. So, for a six-membered ring, it typically produces a cyclohexane ring minus the hydrogen atoms. However, by holding down the ALT key and clicking in the 3D Viewer, an aromatic ring was added directly. Other part of the molecule were attached to the ring by selecting the element in the dropdown list under 'Element used to sketch" arrow. The cursor was moved over one of the carbon atoms in the 3D Viewer. When the atom changed colour to light blue, it was clicked on it. The cursor was moved away to sprout a bond. It was clicked again to place the other atoms i.e thiomethyl group. Substituent are attached to appropriate position to create the quinoline derivative (eg 6-thiomethylquinoline etc.). The ESC key was pressed to cancel further drawing (Materials Studio 8, 2017).

The change in colour of the carbon atom as the cursor moves over it indicates that the carbon can be selected. After attaching all the required atoms to the molecule, the final step was to add the hydrogen atoms by clicking the Adjust Hydrogen button on the toolbar. The Adjust Hydrogen tool automatically fills up any empty valences in a structure with hydrogen atoms to satisfy them. The sketched structure needs to be cleaned by using the Clean tool to tidy up the geometry [10].

2.2.2 Optimization of the Molecules

The sketched molecules will not have an accurate geometry, so all molecules were subjected to geometry optimization to refine the geometry of their structures so as to minimize their torsional and conformational energies as well as global minimum energy of the molecules. This was achieved using the $DMol^3$ geometry optimization task in Accelrys Material Studio 8.0. The access to the $DMol^3$ optimization dialog box which allows the set up and displays the parameters that control the simulation in a $DMol^3$ optimization dialog task was traced either through the menu or through the Modules toolbar. The $DMol^3$ toolbar on the Modules toolbar was clicked and Calculation from the dropdown list/task bar was selected to display the $DMol^3$ calculation dialog box where the following properties; task: geometry optimization, quality: fine were selected, which set the geometry optimization convergence thresholds for any change, maximum force and minimum displacement between optimization cycles. The optimization stopped when the energy convergence was satisfied, along with either the displacement or gradient criteria [11]. If the calculated initial gradients were below the threshold, the optimization will successfully stop without making a single step and without comparing displacements and energies. Three sets of convergence thresholds were available; coarse, medium and fine. The fine was selected which have values of 1×10^{-5} energy (Hartree), maximum force (Hartree $Å^{-1}$) of 0.002 and maximum displacement (Å) of 0.05. The use symmetry box was checked, indicating that the symmetry information was used in the calculation, while spin unrestricted box which searches for spin unrestricted solution was not checked. The exchange correlation functional theory level, LDA was selected followed by the PWC local density functional to be used was also selected. The geometry optimization was conducted and the optimized structures were saved for further use in quantum calculations of some structural and electronic properties [12]. The following are the parameters to be assessed:

HOMO (at orbital number), LUMO (at orbital number), Molecular Mass (g/mol), Dipole Moment (Debye), E_{HOMO} (eV), E_{LUMO} (eV), Gap Energy (ΔE) (eV), Ionization Potential (IP) (eV), Electron Affinity (EA) (eV), Global Hardness (η) (eV), Global Softness (σ) $(eV)^{-1}$, Absolute Electronegativity (χ) (eV), Chemical Potential (μ) (eV), Global Electrophilicity Index (ω) (eV), Nucleophilicity Index (ε) $(eV)^{-1}$, Electron Donating Power (ω^-) (eV), Electron Accepting Power (ω^+) (eV), Net Electrophilicity ($\Delta\omega^{\pm}$) (eV), Energy of Back Donation ($\Delta E_{b\text{-}d}$) (eV), Total Number of Electrons, Fraction of Electrons Transferred (ΔN).

2.2.3 Calculation of the Quantum Chemical Parameters

The electronic structure of the molecules, including the distribution of frontier molecular orbitals E_{HOMO} and E_{LUMO}, Fukui indices were assessed, with a view to establishing the active sites as well as local reactivity of the molecule. The simulations were performed by means of the Density Functional Theory (DFT) electronic program $DMol^3$ using the Mulliken population analysis in the Material Studio 8.0 software. $DMol^3$ permits analysis of the electronic structures and energies of molecules, solids and surfaces using DFT. Electronic parameters for the simulations include restricted spin polarization using the DND basis set and the Perdew Wang local correlation density functional. Local reactivity of the studied compounds was analysed by means of the Fukui indices (FI) to assess regions of nucleophilic and electrophilic behaviour [13]. The electronic and structural properties of a sketched molecule was requested through the Properties tab of the $DMol^3$ calculation dialog. These properties were computed as part of the calculation and viewed using the $DMol^3$ Analysis dialog. The properties that can be accessed through the Properties tab include: band structure, density of states (DOS), electron densities, frequencies, Fukui functions, optics, orbitals and population analysis (Materials Studio 8, 2017).

2.2.4 Quench Molecular Dynamic Simulation

One common molecular dynamics method, called quench molecular dynamics, perform a standard molecular dynamics calculation with an additional geometry optimization step, in which a geometry optimization is performed on every frame in the trajectory file. Effectively, molecular dynamics is used to sample many different low energy configurations (Materials Studio 8, 2017).

In this work, Forcite Plus were used to perform molecular dynamics on a system comprising organic molecules (The quinoline derivatives), and a metal (aluminium) surface. The aluminium surface was cleaved from the rutile form of the aluminium crystal structure [14]. The molecule was placed on the surface, optimized before quench molecular dynamics was ran. A study table was used to look for the lowest energy conformation and finally was also used to calculate the binding energy which is the ultimate target (Materials Studio 8, 2017).

3.0 RESULTS AND DISCUSSIONS

In order to study the effect of the molecular structure on inhibition efficiency, quantum chemical calculations with complete geometry optimizations of the corrosion inhibitors was performed using DMol3 module of Materials Studio software version 8.0

(BIOVIA, Accelrys) 2017. This module is an atomic orbital implementation of density functional theory (DFT) in the local density approximation (LDA) regime. Calculations were done in the Perdew-Wang Correlation (PWC) form, at the double numerical quality plus d-functions (DND) atomic basis set level. Complete geometrical optimizations of all the quinoline structures, the electron density, the highest occupied molecular orbital (HOMO), and the lowest unoccupied molecular orbital (LUMO) were obtained as shown below in figure 4,5 and 6:

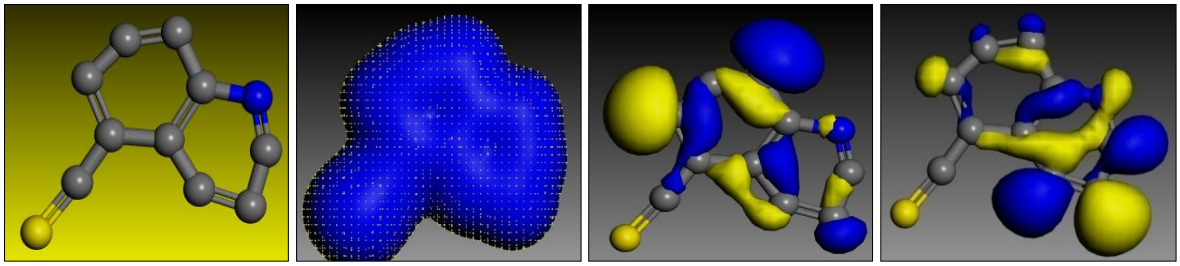

Figure 4: Optimized structure, electrondensity, HOMO and LUMO of 5-TMQ

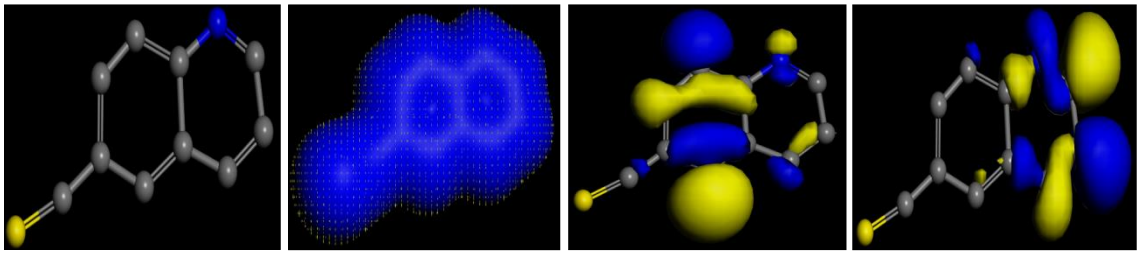

Figure 5: Optimized structure, electrondensity, HOMO and LUMO of 6-TMQ

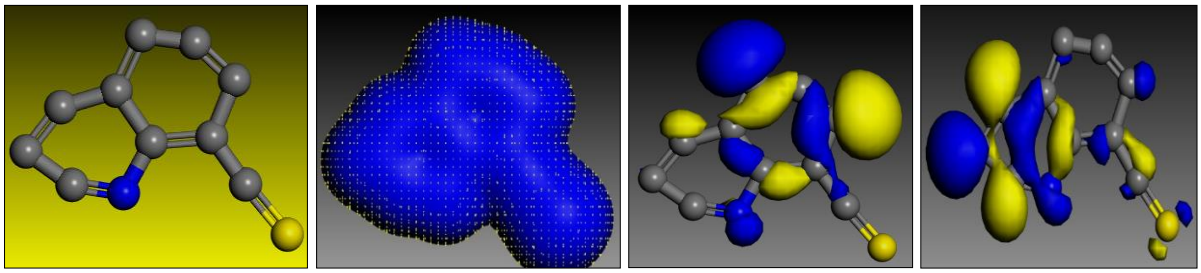

Figure 6: Optimized structure, electrondensity, HOMO and LUMO of 8-TMQ

Table 1: The Values of electronic parameters and Eigen values of 5-TMQ, 6-TMQ and 8-TMQ

Electronic/structural property	5-TMQ	6-TMQ	8-TMQ
HOMO (at orbital number)	82	82	82
LUMO (at orbital number)	83	83	83
E_{HOMO} (eV)	-6.047	-6.002	-5.887
E_{LUMO} (eV)	-4.468	-4.415	-4.525
ΔE (eV)	1.595	1.587	1.362
Molecular mass (g/mol) $C_{10}H_7NS$	173	173	173
Ionization potential (*IP*) (eV)	6.047	6.002	5.887
Electron affinity (*EA*) (eV)	4.468	4.415	4.525
Absolute/Global hardness (η)	0.789	0.794	0.881
Global softness (σ)	1.267	1.259	1.468
Absolute electronegativity (χ)	5.258	5.209	5.206
Total number of electrons	83	83	83
Fraction of electrons transferred (ΔN)	0.109	0.246	0.289
Energy of back donation ($\Delta E_{b\text{-}d}$)	-0.197	-0.199	-0.171
Chemical Potential (μ) (eV)	-4.436	-6.633	-7.266
Electrophilicity Index (ω) (eV)	21.03	18.239	16.610
Nucleophilicity (ε) (eV)−1	0.052	0.062	0.098
Electron Accepting Power ($\omega+$) (eV)	24.201	23.413	20.412
Electron Donating Power ($\omega-$) (eV)	42.138	49.603	53.081

Net Electrophilicity ($\Delta\omega\pm$) (eV)	63.339	53.016	49.493

Quantum chemical calculations were performed in order to gain insights at the molecular level, electron distribution of the different inhibitor molecules used as well as to understand the nature of their interactions with the aluminium surfaces [15]. The first consideration was to assess the electronic structures of the molecules, including the distribution of frontier molecular orbitals and Fukui indices, with a view to establish the active sites as well as local reactivity of the molecules [16]. In this research, 5, 6 and 8-thiomethylquinolines are employed as the aluminium corrosion inhibitors tested theoretically in acid medium. The quantum chemical calculations for electronic and structural properties are shown in tables 1 of same substituent attached to the core quinoline. The most popular parameters which play a prominent role are the eigen values of the highest occupied molecular orbital (HOMO) and lowest unoccupied molecular orbital (LUMO), the HOMO-LUMO gap (ΔE), chemical hardness and softness, electro-negativity and the number of electrons transferred from inhibitor molecule to the metal surface [17].

E_{HOMO} Represents the energy of the highest occupied molecular orbital. It indicates the ability of a molecule to donate electrons (nucleophilicity). Higher E_{HOMO} values imply better electron-donating ability [17]. According to the frontier molecular orbital theory (FMO) of chemical reactivity, transition of electron is due to an interaction between HOMO (highest occupied molecular orbital) and LUMO (lowest unoccupied molecular orbital) of reacting species. The energy of HOMO is directly related to the ionization potential and characterizes the susceptibility of the molecule toward attack by electrophiles. Higher values of E_{HOMO} are likely to indicate a tendency of the molecule to donate electrons to appropriate acceptor molecules with low energy or empty electron orbital [17].

E_{LUMO} Represents the energy of the lowest unoccupied molecular orbital. Indicates the ability of a molecule to accept electrons (electrophilicity) [17]. Lower E_{LUMO} values imply better inhibition efficiency, as the molecule can accept electrons from the metal surface.

$\Delta E = E_{LUMO} - E_{HOMO}$ Represent energy gap [18]. A smaller gap indicates easier electron transfer, facilitating corrosion inhibition. E_{HOMO}: Higher values suggest better inhibition efficiency, as the molecule can donate electrons to the metal surface. E_{LUMO}: Lower values indicate better inhibition efficiency, as the molecule can accept electrons from the metal surface. Higher E_{HOMO} and lower E_{LUMO} values typically correspond to better corrosion inhibition efficiency [18]. A smaller ΔE (gap energy) indicates a more effective corrosion inhibiton. Among the three molecules used as aluminium corrosion inhibitors in this study, the molecule with higher E_{HOMO} and low **E_{LUMO}** is 8-TMQ. All the molecules used here inhibits the aluminium corrosion to high extent, but 8-TMQ here displays superior inhibition efficiency comparatively.

Global Hardness (η):

Measures the resistance to electron density changes. Higher η indicates a harder molecule, less prone to polarization [19]. The values of global hardness obtained here in table 1 is relatively high for almost all the molecules but higher in 8-TMQ. This shows that the 8-TMQ molecule functions effectively without undergoing any polarization which may hinder performance. Global Softness (σ) is the inverse of global hardness. Higher σ indicates a softer molecule, more prone to polarization.

Nucleophilicity:

Measures the ability to donate electrons. Higher nucleophilicity indicates better electron-donating ability [20]. The molecule 8-TMQ showed higher nucleophilicity. This indicated direct confirmation of its better performance as inhibitor for aluminium corrosion.

Electrophilicity:

Measures the ability to accept electrons. Higher electrophilicity indicates better electron-accepting ability [20]. 8-TMQ has the least electrophilicity among the three molecules.

Ionization Potential (IP):

The energy required to remove an electron. Lower IP indicates easier electron removal. Table1. Shows that IP = 8-TMQ < 6-TMQ < 5-TMQ in order of increasing ionization potential comparatively.

Electron Affinity (EA):

The energy released when an electron is added. Higher EA indicates easier electron addition. Table1 revealed that all the molecules used here have electron affinity, but 8-TMQ exhibits the highest [20].

Absolute Electronegativity (χ):

A measure of the tendency to attract electrons. Higher χ indicates higher electronegativity [21]. From the table 1,8-TMQ have highest values of (χ).

Chemical Potential (μ):

Measures the tendency of a molecule to gain or lose electrons. Lower μ indicates a higher tendency to gain. Generally the table 1shown the correlation between the chemical potential of each molecule and its aluminium corrosion inhibition performance [21].

Nucleophilicity Index (ε):

A dimensionless parameter indicating nucleophilicity. Higher ω indicates better nucleophilicity [22]. There is a strong correlation between the value of ω and corrosion inhibition of each

of the molecules as shown in table 1 above. 8-TMQ exhibit higher $\boldsymbol{\varepsilon}$ comparably.

Electrophilicity Index ($\boldsymbol{\omega}$):

A dimensionless parameter indicating electrophilicity. Higher ω indicates better electrophilicity [22]. The electrofilicity index of each of the above hydroxy-quinolines tested here as corrosion inhibitors for aluminium is approximately related to the performance of each molecule as indicated in table 1 above.

Electron Accepting Power ($\boldsymbol{\omega^+}$):

Measures the ability of a molecule to accept electrons. Higher ω^+indicates better electron-accepting ability, enhancing corrosion inhibition. **Electron Donating Power ($\boldsymbol{\omega^-}$)**: Measures the ability of a molecule to donate electrons. Higher ω^-indicates better electron-donating ability, enhancing corrosion inhibition [23]. The molecule 8-TMQ exhibit higher electron donating power (ω^+) as shown in the table 1 above. **Net Electrophilicity ($\Delta\boldsymbol{\omega^{\pm}}$)**: A comprehensive measure of electrophilicity, considering both electron-accepting and donating abilities. Higher $\Delta\omega^{\pm}$ indicates better overall electrophilicity, enhancing corrosion inhibition [24]. This is in agreement with what was obtained as shown in tables 1 for all the quinoline derivatives used here.

Energy of Back Donation ($\Delta\boldsymbol{E_{b-d}}$):

Measures the energy associated with the back-donation of electrons from the metal surface to the inhibitor molecule. It indicates the strength of the feedback bond between the metal and inhibitor [25]. Lower energy values indicate stronger back-donation, enhancing corrosion inhibition. It stabilizes the metal-inhibitor complex, reducing metal reactivity. There is low values of energy of back Donation for all the molecules as indicated in table 1 above.

Fraction of Electron Transferred ($\Delta\boldsymbol{N}$):

Measures the extent of electron transfer between the inhibitor and metal surface. It indicates the degree of charge transfer and covalent bonding. Higher ΔN values indicate more electron transfer, enhancing corrosion inhibition. ΔN facilitates the formation of a protective layer on the metal surface [26]. Generally there are adequate number of electrons transferred between the inhibitors and the metal for all the molecules used in this research. This has justified the inhibition performance of all the thiomethylquinoline molecules used as corrosion inhibitors for aluminium.

4. Quench Molecular Dynamic Simulation

The statistical table 2 provide insights into the electronic parameters of different quinoline derivatives based on the values of K:H−(I+J)K : H-(I+J)K:H−(I+J). Key statistical metrics such as range, mean, median, variance, standard deviation, skewness, and kurtosis have been used to describe the electronic behaviour of each molecule.

Table 2: The Statistical information for confirmation of electronic parameters of 5-TMQ, 6-TMQ and 8-TMQ

	5-TMQ	6-TMQ	8-TMQ
	K : H-(I+J)	K : H-(I+J)	K : H-(I+J)
Number of sample points	3	3	3
Range	2.510460e-006	2.336200e-005	1.533460e-005
Maximum	-39.92454065	-41.54536867	-43.52989638
Minimum	-39.92454316	-41.54539203	-43.52991171
Mean	-39.92454159	-41.54538381	-43.52990181
Median	-39.92454095	-41.54539073	-43.52989733
Variance	1.251300e-012	1.149030e-010	4.921390e-011
Standard deviation	1.370020e-006	1.312840e-005	8.591910e-006
Mean absolute deviation	1.048110e-006	1.009380e-005	6.603900e-006
Skewness	-0.36362900	0.38064700	-0.37959600
Kurtosis	-2.33333000	-2.33333000	-2.33333000

From the table 2 the range of values varies significantly across the quinoline derivatives. The 5-TMQ, 6-TMQ, and 8-TMQ show extremely small ranges (in the order of 2.5 or lower), suggesting very stable electronic properties. The mean and median values are very close for all the compounds, suggesting a symmetric distribution of data [27].

Skewness measures the asymmetry of the distribution. The 5-TMQ and 8-TMQ exhibit negative skewness, suggesting a longer left tail. Most values are close to zero, meaning the data is fairly symmetric [28]. Table 2 also show that kurtosis values are consistently around -2.333, suggesting a platykurtic distribution (flatter than a normal distribution). This means the data distributions are broad and have fewer extreme values (outliers) [29]. The Large variance and standard deviation indicate significant dispersion, meaning the electronic parameters fluctuate widely. Low variance suggests very little variation, meaning highly stable electronic properties. The 5-TMQ, and 6-TMQ and compounds have very low range and variance, this has

justified their stable electronic properties. This stability could make them more predictable for applications requiring consistent electronic behavior [29]. For Corrosion Inhibition: Stable electronic parameters may indicate consistent adsorption behavior, making these derivatives (5-TMQ, 6-TMQ and 8-TMQ) better corrosion inhibitors. For Electronic Applications, 5-TMQ and 6-TMQ, could be useful in applications where consistent electronic properties are required over to Low variance and high stability [29].

Table 3: The Values of adsorption parameters for the interaction of 5-TMQ, 6-TMQ and 8-TMQ with the Al (110) surface

Adsorption properties (kcal/mol)	5-TMQ	6-TMeQ	8-TMQ
Total kinetic energy	8.87135293	19.82236135	19.82236135
Total potential energy	27.30652070	23.03870692	36.76947069
Energy of molecule	67.23106165	64.58407559	80.29938240
Energy of Al(110) surface	0.00000000	0.00000000	0.00000000
Adsorption energy	-39.92454095	-41.54536867	-43.52991171

The binding energy (E_{bind}) between the metal surface and the inhibitor molecules are presented on Tables 3. To quantitatively estimate the interaction between each aminoquinoline and the aluminium surface, the adsorption/binding energy, (E_{ads} / E_{bind}), was calculated using Equation: Binding Energy = E_{total} – ($E_{inhibitor}$ + $E_{Al\ surface}$). In each case, the potential energies were calculated by averaging the energies of each structure's lowest energy. As can be seen from the data, the binding (adsorption) energies are all negative suggesting stable adsorption structures [30]. However, the magnitude of the calculated binding energies is < 100 kcal mol^{-1}. This is despite the fact that the simulations did not take into consideration the specific covalent interactions between the molecules and the Al surface. This has been reported by [30], to be in the range of physisorptive interactions. From the Table 3, it is observed that the binding energies for the quinoline molecules on Al (110) slab are of the magnitude between -39.20 to -43.7 (kcal mol^{-1}). This implies that the molecules are partly adsorbed on the Al surface. A detailed analysis of the on-top view of the adsorbed molecules on Al (110) emphasizing the soft epitaxial adsorption mechanism with accommodation of the molecular backbone in characteristic epitaxial grooves on the metal surface [31].

5. Fukui Indices

The sites at which an atom can bind to the metal surface is very important in corrosion studies. The figures in the prentices are the positions of each atom in the molecule, and the values outside are the extent of nuleophilic or electrophilic interaction of the atom with the aluminium surface as shown in table 4 below.

Table 4: Sites for Electrophilic and Nucleophilic Attack

Molecule	Electrophilic (F^-)				Nucleophilic (F^+)			
	Mulliken		Hirshfeld		Mulliken		Hirshfeld	
	Atom	Value	Atom	Value	Atom	Value	Atom	Value
5-TMeQ	C (04)	0.100	C (04)	0.090	C (04)	0.100	C (04)	0.091
	C (06)	0.090	C (05)	0.085	C (06)	0.090	C (05)	0.085
	C (10)	0.090	N (03)	0.083	C (09)	0.090	N (03)	0.083
	S (05)	0.154	S (05)	0.147	S (04)	0.153	S (05)	0.146
	C (10)	0.112	C (08)	0.100	C (10)	0.112	C (10)	0.100
6-TMeQ	C (04)	0.100	C (04)	0.090	C (04)	0.100	C (04)	0.091
	C (06)	0.090	C (05)	0.085	C (06)	0.090	C (05)	0.085
	C (10)	0.090	S (06)	0.083	C (09)	0.090	N (03)	0.083
	S (06)	0.154	C (04)	0.147	S (06)	0.153	S (05)	0.146
	C (07)	0.112	C (10)	0.100	C (10)	0.112	C (08)	0.100
8-TMeQ	C (04)	0.100	C (04)	0.090	C (04)	0.100	C (04)	0.091
	C (06)	0.090	C (05)	0.085	C (06)	0.090	C (05)	0.085
	C (09)	0.090	N (03)	0.083	C (09)	0.090	N (07)	0.083
	S (08)	0.154	S(08)	0.147	S (08)	0.153	S (08)	0.146
	C (09)	0.112	C (10)	0.100	C (10)	0.112	C (07)	0.100

The Fukui functions shown in the table 4 are derived from Density Functional Theory (DFT) calculations and provides insight into how electron density redistributes when adding or removing an electron [31]. The local reactivity of the inhibitor molecules was analyzed through the evaluation of Fukui indices. The condensed Fukui functions allowed us to distinguish each part of the molecule on the basis of its distinct chemical behaviour due to different functional group or substituent [32]. Thus, the site for nucleophilic attack will be the place where the value of F^+ is a maximum and the site for electrophilic attack will be the place where the value of F^- is maximum [32].

The values of the Fukui functions for a nucleophilic and electrophilic attack for all the inhibitors as given in Table 4 (for the nitrogen the carbon atoms). Inspection of the values of Fukui functions presented shows that the quinoline derivatives have propitious zones for nucleophilic cattack located on (C and N). The HOMO location on each molecule agrees with the atoms that exhibit greatest values of indices of Fukui, both indicated the zones by which the molecule would be adsorbed on the aluminium surface [33].

Electrophilic Attack Susceptibility:

This measures the change in electron density when an electron is added to the system. High values electrophilic attack susceptibility indicate regions that are more susceptible to electrophilic attack. In quinoline derivatives, this is crucial for understanding interactions with electrophilic species, such as protons or metal ions [33]. Nucleophilic Attack Susceptibility: This measures the change in electron density when an electron is removed from the system. High values of nucleophilic attack susceptibility indicate sites where nucleophiles are likely to attack. This is particularly useful in studying quinoline derivatives' interactions in redox reactions [34].

For the 5-TMQ, 6-TMQ, and 8-TMQ, the presence of the thiomethyl group slightly modifies the electron density distribution, affecting reactivity. Typically, the thiomethyl groups donate electron density, making adjacent positions more susceptible to electrophilic attack.

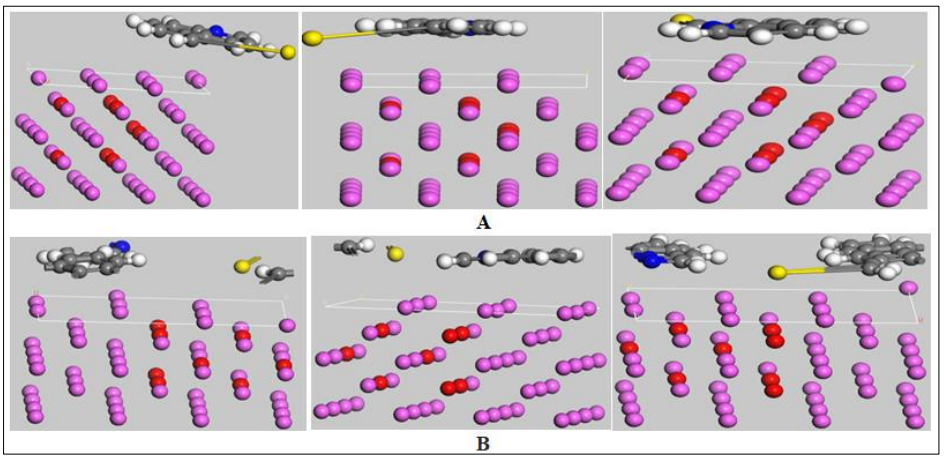

Figure 7: The final side snapshots of adsorbed 5-TMQ, 6-TMQ and 8-TMQ molecules, from left to right respectively, on aluminium (110) reflection. (A) Single molecules. (B) Many molecule

Further information on the interaction between the inhibitors and the aluminium surface can be provided by the molecular dynamics simulations. From left to right indicate (A) Single molecules and (B) Many molecule respectively, on aluminium (110) reflection.

The adsorption of quinoline derivatives molecules on the aluminium surfaces were analyzed at a molecular level by molecular dynamics simulations, using Forcite quench molecular dynamics to sample many different low energy configurations and to identify the low energy minima [35]. As shown in figure 7, the optimized molecules were used for the simulation. Solvent and charge effects were neglected in all the simulations and calculations were performed at the metal/vacuum interface. Although this is clearly an over simplification of the actual situation, it is adequate to qualitatively illustrate the differences in the adsorption behaviour of the molecules and provide sufficient insight to the study objectives [36].

Figures 7: shows representative snapshots of the cross-section of the lowest energy adsorption configurations for the single molecules on the Al (110) surface from the top (A) and for more than one molecule from the bottom (B). The molecules can be seen to maintain a flat-lying adsorption orientation on the metal surface thereby maximizing contact and enhancing the degree of surface coverage. This parallel adsorption orientation also facilitates interaction of π - electrons of the quinoline nucleus and the heteroatoms (N and S) in the molecules with the metal surfaces [37].

5.0 CONCLUSION

The study of the quantum chemical parameters, the adsorption parameters from the simulation of the molecules, the Mulliken and Hirshfeld values of the fukui indices for the three molecules of thiomethylquinolines (5-TMQ, 6-TMQ, and 8-TMQ) shown that all the three molecules exhibits very high potential for inhibition of aluminium corrosion in HCl environment. However, 8-TMQ is superior to 5-TMQ and 6-TMQ. The difference in the quantum chemical properties responsible for high inhibition efficiency shown by the molecules despite having the same mass and structure is believed to come from orientation of the thiomethyl substituent ($-SCH_3$) position on the parent quinoline molecule. Intra-molecular interaction is suspected to occurred in 5-TMQ and 6-TMQ which leads to poor donation of free electron from the entire molecule

in the formation of the metal-inhibitor complex. The stronger the intra-molecular interaction, the slower the complex formation hence reduced inhibition efficiency. Thiomethyl group at position eight do not likely form intra-molecular interaction, as a result, 8-TMQ readily form complex with the aluminium and displayed excellent properties for higher corrosion inhibition performance than other two molecules. Corrosion inhibition efficiency of heterocyclic compound can be influence by the position of substituent attached to the parent molecule.

6. List of Abbreviations

Abbreviations Meaning

5-TMQ 5-thiomethylquinoline
6-TMQ 6-hiomethylquinoline
8-TMQ 8-hiomethylquinoline
DFT density functional theory
MD molecular dynamic

7. Declaration: The authors declared that there is no conflicts of interest.

REFERENCES

1. Abeng, F. E., Anadebe, V., Nkom, P. Y., Uwakwe, K. J., & Kamalu, E. G. (2022). Experimental and theoretical study on the corrosion inhibitor potential of quinazoline derivative for mild steel in hydrochloric acid solution. *Journal of Electrochemical Science and Engineering*, 12(3), 243–257.
2. Abiola, O. K., Oforka, N. C., & Ebenso, E. E. (2004). The inhibition of mild steel corrosion in an acidic medium by fruit juice of Citrus paradisi. *Journal of Corrosion Science and Engineering, 5*(1), 1-8.
3. Achebe, C. H., Okafor, P. C., & Oguzie, E. E. (2012). Corrosion inhibition of mild steel in hydrochloric acid by acid extract of *Garcinia kola* seed. *International Journal of Materials and Chemistry*, 2(4), 158–164.
4. Adejo, A. O., et al. (2012). Corrosion inhibition of mild steel in HCl by ethanol extract of *Dacryodis edulis* leaves. *Journal of Emerging Trends in Engineering and Applied Sciences*, 3(2), 306–311.ScienceDirect
5. Adejo, A. O., et al. (2012). Water extracts of cassava leaf as corrosion inhibitor for mild steel in sulfuric acid solution. *Journal of Chemical and Pharmaceutical Research*, 4(2), 1220–1226. jocpr.com
6. Beltrán-Prieto, C., Serrano, A. A. A., Solís-Rodríguez, G., Martínez, A., Orozco-Cruz, R., Espinoza-Vázquez, A., & Miralrio, A. (2022). A General Use QSAR-ARX Model to Predict the Corrosion Inhibition Efficiency of Commercial Drugs on Steel Surfaces. *International Journal of Molecular Sciences*, 23(9), 5086. pmc.ncbi.nlm.nih.gov
7. Bostan, R., & Popa, A. (2012). Evaluation of some phenothiazine derivatives as corrosion inhibitors for bronze in weakly acidic solution. *Journal of Applied Electrochemistry*, 42(4), 321–328.ResearchGate
8. Brycki, B., Szulc, A., Kowalczyk, I., & Koziróg, A. (2017). Organic corrosion inhibitors. *International Journal of Corrosion and Scale Inhibition*, 6(4), 354–372.
9. Chavan, N. D., & Vijayakumar, V. (2024). Synthesis, DFT Studies on a Series of Tunable Quinoline Derivatives. *RSC Advances*, 14(29), 21089–21101. https://doi.org/10.1039/D4RA03961K
10. Chi, M. and Zhao, Y.P. (2009). Adsorption of formaldehyde molecule on the intrinsic and Al-doped grapheme: A first principle study. Computional Materials Science, 48:1085–1090.
11. Dai W., and Zhang, Y.Y. (2012). Molecular dynamics simulation of the adsorption behaviour of amino acid corrosion inhibitor on Cu (1 0 0) surface. Applied Mechanics and Materials, 121-126: 226-230.
12. Ebenso, E. E., et al. (2010). Corrosion inhibition and adsorption properties of ethanol extract of *Gongronema latifolium* on mild steel in H_2SO_4. *Portugaliae Electrochimica Acta*, 28(1), 13–22. ResearchGate
13. Eddy, N. O. (2008). Inhibitive and adsorption properties of ethanol extract of Musa sapientum peels as a green corrosion inhibitor for mild steel in H_2SO_4. *African Journal of Pure and Applied Chemistry*, 2(6), 46–54.
14. Elfaydy M., Lgaz H., Salghi R., Larouj M., Jodeh S., Rbaa M., Oudda H., Toumiat K. and Lakhrissi B. (2016) " Investigation of corrosion inhibition mechanism of quiniline Derivative on Mild steel in 1.0M HCl Solution : Experimental, Theoretical and Monte Carlo simulation, *Journal of material and Environmental Science.* Vol. 7(9) 3193-3210, ISSN: 2028-25086.
15. El-HassanAssiri Majid Driouch, Jamila LazrakZakariae, Bensouda Ali Elhalouiand Mouhcine Sfaira (2020) . Development and validation of QSPR models for corrosion inhibition of carbon steel by some pyridazine derivatives in acidic medium, Heliyon, Vol.15, 50-67
16. Fragoza-Mar,. (2012). Corrosion inhibitor activity of 1,3-diketone malonates for mild steel in aqueous hydrochloric acid solution. *Corrosion Science*, 61, 171–184.
17. Felipe, O. M., Cavalcanti, E. B., & Navarro, M. (2013). Evaluation of *Croton cajucara* extract as a corrosion inhibitor for carbon steel in saline medium. *Electrochimica Acta, 97*, 167-175.
18. Fu, J., Li, S., & Wang, Y. (2020). Computational and electrochemical studies of some amino acid compounds as corrosion inhibitors for mild steel in hydrochloric acid solution. *Journal of Molecular Liquids*, 309, 113102.Google Scholar

19. Goyal, M., Kumar, S., Bahadur, I., Verma, C., & Ebenso, E. E. (2018). Organic corrosion inhibitors for industrial cleaning of ferrous and non-ferrous metals in acidic solutions: A review. *Journal of Molecular Liquids*, 256, 565–573.
20. James, A. O., & Akaranta, O. (2014). The inhibition of corrosion of zinc in 2.0 M hydrochloric acid solution with acetone extract of red onion skin. *African Journal of Pure and Applied Chemistry*, 3(11), 212–217.SCIRP_SCIRP
21. Jun, J. V., Petersson, E. J., & Chenoweth, D. M. (2018). Rational Design and Facile Synthesis of a Highly Tunable Quinoline-Based Fluorescent Small-Molecule Scaffold for Live Cell Imaging. *Journal of the American Chemical Society*, 140(30), 9486–9493. https://doi.org/10.1021/jacs.8b03738
22. Kadapparambil Sumithra, Kavita Yadav, Manivannan Ramachandran and Noyel Victoria Selvam (2017b). Electrochemical investigation of the corrosion inhibition mechanism of *Tectona grandis* leaf extract for SS304 stainless steel in hydrochloric acid, *De Gruyter,*DOI 10.1515/corrrev-2016-0074
23. Khaled, K. F., Sherif, E. M., & Hamed, F. (2016). Effect of cerium chloride on corrosion inhibition of aluminum in seawater. *Journal of Applied Electrochemistry, 46*(3), 187-197.
24. Nnanna, L. A., Uroh, C. A., & Mejeha, I. M. (2016). Corrosion inhibition efficiency of *Pentaclethra macrophylla* root extract on mild steel in alkaline medium. *Research Journal of Chemical Sciences, 6*(1), 42-50.
25. Olufunmilayo O. Joseph and Olakunle O. Joseph (2020) "Corrosion Inhibition of Aluminium Alloy by Chemical Inhibitors: An Overview, IOP Conference Series: Materials Science and Engineering, Volume 1107
26. Quraishi, M. A., Sardar, R., & Jamal, D. (2007). Corrosion inhibition of aluminium in acid solutions by some imidazoline derivatives. *Materials Chemistry and Physics, 98*(1), 223-226.
27. Rajendran S., J. Jeyasundari, P. Usha, J. A. Selvi, B. Narayanasamy, A. P. P. Regis, and P. Rengan (2013) "Corrosion behaviour of aluminium in the presence of an aqueous extract of Hibiscus Rosa-sinensis," *Portugaliae Electrochimica Acta*, 27 (2), 153–164.
28. Saha S.K. and Banerjee P. A(2015). Theoretical approach to understand the inhibition mechanism of steel corrosion with two aminobenzonitrile inhibitors. *RSC Adv.;*5(87):71120. DOI: https://doi.org/10.1039/C5RA15173B
29. Shehu U. Najib, U. I. Gaya and Muhammad A. A. (2019) . Influence of Side Chain on the Inhibition of Aluminium Corrosion in HCl by α-Amino Acids, King Mongkut's University of Technology North Bangkok.
30. Singh, A., Ebenso, E. E., & Quraishi, M. A. (2016). Corrosion inhibition of carbon steel in HCl solution by some plant extracts. *International Journal of Corrosion and Scale Inhibition, 5*(2), 116-132.
31. Talari M., S.M. Nezhad, S.J. Alavi, M. Mohtashamipour, A. Davoodi, S. Hosseinpour, (2019). Experimental and computational chemistry studies of two imidazole-based compounds as corrosion inhibitors for mild steel in HCl solution, J. Mol. Liq. 286 110915, https://doi.org/10.1016/j.molliq.2019. 110915.
32. Verma, C., Ebenso, E. E., Quraishi, M. A., & Hussain, C. M. (2021). Recent developments in sustainable corrosion inhibitors: design, performance and industrial scale applications. *Materials Advances*, *2*(11), 3806–3830.
33. Verma, C., Olasunkanmi, L. O., Obot, I. B., Ebenso, E. E., & Quraishi, M. A. (2016b). 5-Arylpyrimido-[4,5-b]quinoline-diones as new and sustainable corrosion inhibitors for mild steel in 1 M HCl: a combined experimental and theoretical approach. *RSC Advances*, 6(19), 15639–15654. https://doi.org/10.1039/C5RA27417F
34. Zhang, D.-Q., Gao, L.-X., & Zhou, G.-D. (2008). Inhibition of copper corrosion by bis-(1,1-dimethyl-ethyl)-dithiocarbamate in aerated hydrochloric acid solutions. *Materials Chemistry and Physics*, 112(2), 353–358.
35. Zhao, P., Wang, Y., & Li, Y. (2017). Corrosion inhibition of aluminum alloy in hydrochloric acid solution by triazinedithiol inhibitors. *Journal of Molecular Liquids*, 225, 602-611.
36. Zhao, T., Li, X., Zhang, S., & Hou, B. (2017). Adsorption and inhibition effect of organic inhibitors on mild steel corrosion in acid medium. *Corrosion Science, 125*, 255-265.
37. Zhu C., H. X. Yang, Y. Z. Wang, D. Q. Zhang, Y. Chen, and L. X. Gao (2018), "Synergistic effect between glutamic acid and rare earth cerium (III) as corrosion inhibitors on AA5052 aluminum alloy in neutral chloride medium," Ionics, vol. 25, no. 3, pp. 1395–1406.